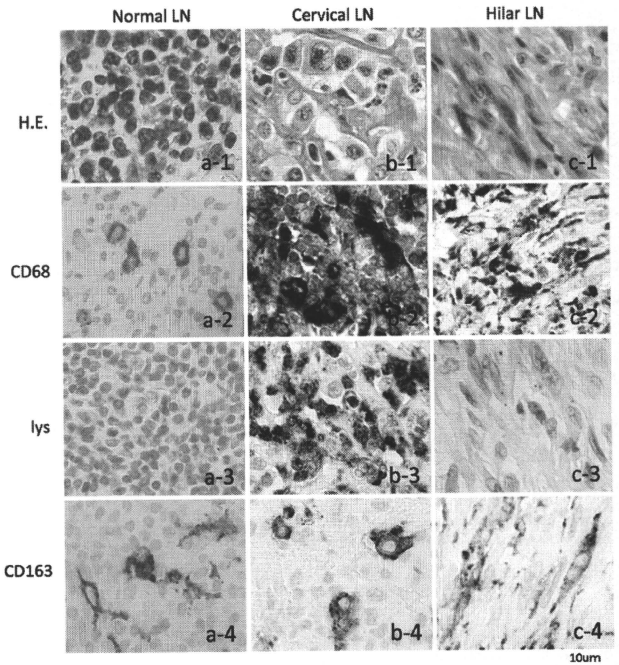

Fig. 1 Histopathologic features of the normal (*a*), cervical (*b*) and right hilar (*c*) lymph node (LN), with H&E staining, CD68, lysozyme (Lys) and CD163 immunohistochemical staining (*a-1*). There were macrophages with abundant cytoplasm in normal LN. *a-2*, *a-3*, *a-4* Macrophages were positive for CD68 and CD163, but negative for lysozyme. *b-1* Large atypical cells with abundant cytoplasm in cervical LN. *c-1* Spindle-shaped cells in hilar LN. *b-2*, *c-2* Neoplastic cells were diffusely positive for CD68. *b-3* A part of tumor cells with small cytoplasm were positive for lysozyme. *b-4* CD163 was sporadically positive in tumor cells with abundant cytoplasm or spindle-shaped. *c-3* Tumor cells were negative for lysozyme. *c-4* Tumor cells with spindle shape were diffusely positive for CD163

In 1993, right hilar lymphadenopathy was noted, but etiology was equivocal by transbronchial lung biopsy. The lymph node size (17 mm in diameter) remained unchanged for a long time, but it enlarged gradually in the last several months. Computed tomography (CT) revealed lymphadenopathy on the left neck, right hilar, and tracheal bifurcation areas. Fluorodeoxyglucose-positron emission tomography (FDG-PET) examination integrated with CT scanning showed elevated FDG uptake on the lymph nodes of the left cervical, right hilar, and tracheal bifurcation areas, left tonsil, and stomach. No other symptoms, such as general fatigue, fever, weight loss, and night sweat were noted. Complete blood count showed anemia at hemoglobin level of 80 g/L, white blood cell count of 5.6 $\times$ 10^9/L (68% granulocytes, 19% lymphocytes, 12% monocytes), and platelet count of 450 $\times$ 10^9/L. Serum biochemistry studies revealed AST 109 IU/L, ALT 138 IU/L, LD 121 IU/L, sIL-2R 868 IU/mL, and CRP 7.16 mg/dL. Bone marrow aspirate examination showed no evidence of tumor infiltration and hemophagocytosis. Left cervical lymphadenectomy was subsequently performed. The pathological analysis of the lesion displayed infiltration of large atypical cells with abundant cytoplasm (Fig. 1b-1). No emperipolesis and hemophagocytosis were observed. Immunohistochemistry revealed that the majority of tumor cells were negative for LCA (PD7/26, 2B11), CD3 (F7.2.38), CD1a (MTB1), CD20 (L26), CD21 (IF8), CD35 (RLB25), CD79a (JCB117), and S-100 protein (polyclonal), and were positive for CD68 (KP-1) and lysozyme (polyclonal) with a sporadic positive staining of CD163 (10D6) (Fig. 1b). On careful assessment, the tumor cells were noted to consist of two immunohistopathologically distinct populations: (A) oval CD68+lysozyme+CD163− cells and (B) abundant cytoplasm or spindle-shaped CD68+lysozyme−CD163+ cells (Fig. 1b). The cervical lymph node was infiltrated mainly by population (A) with sporadic (B). Clonal gene rearrangements in TCR Cβ1, TCRγJ, and IgH were not detected by southern blotting. Based on these histopathological, immunohistochemical, and genetic findings, he was diagnosed to have HS. Upper gastrointestinal tract endoscopy (GIS) showed the

protruded lesion of the greater curvature of the stomach. The tumor involvement was confirmed in the biopsy specimen, which showed cell infiltration with a larger number of population (B), as well as population (A) when compared with the cervical lymph node.

Full-dose CHOP chemotherapy was performed in November 2006. After the first course of CHOP, no FDG uptake on the lymph nodes at the cervical and tracheal bifurcation areas was noted. However, the uptake on the hilar lymph node and the stomach increased. The level of sIL-2R rose to 1400 IU/mL but the tumor size on the stomach as assessed by GIS did not change. Because of anemia due to the gastric bleeding, irradiation therapy to the stomach was performed in January 2007. The size of the gastric tumor reduced and the bleeding stopped. In April 2007, transbronchial lung biopsy was performed because of the rapid enlargement of hilar lymph node. The specimen had characteristic features of HS as assessed by hematoxylin–eosin staining. Irradiation therapy of 42 Gy to the right hilar lymph node was applied, but only slight reduction in size was observed. In June 2007, FDG-PET CT demonstrated persistent FDG uptake on the right hilar lymph node and multiple uptake then appeared in the abdomen and brain.

He was re-admitted because of multiple brain metastases in July 2007. Right after the hospitalization, he developed intestinal perforation. Partial resection of the small intestine and colostomy was urgently performed, but he died of bleeding from multiple intestinal tumors and exacerbation of liver dysfunction after the operation.

An autopsy was performed with the consent of his family. Neoplastic cells infiltrated the stomach, duodenum, small intestine, colon, liver, right adrenal grand, cerebellum, right pulmonary hilar lymph node, and lingual tonsil. There were no emperipolesis and hemophagocytosis in the tumor sites, and no tumor involvement of the bone marrow and spleen. Immunohistochemically, vast majority of tumor cells in the right hilar lymph node were population (B) spindle-shaped CD68+lysozyme−CD163+ cells (Fig. 1c). These cells were Ki-67 (MIB-1)-negative. CD163/Ki-67 double staining on the cervical lymph node was also performed. Ki-67 was sporadically positive only in CD163-negative population (A) and completely negative in CD163-positive population (B) (Table 1). Ki-67 was not a useful marker for the identification of tumor cells in this case.

3 Discussion

The WHO classification divided histiocytic and dendritic cell neoplasms into 6 categories, namely histiocytic sarcoma, Langerhans cell histiocytosis, Langerhans cell sarcoma, follicular dendritic cell sarcoma/tumor, interdigitating cell sarcoma/tumor, and not otherwise specified (NOS). Immunohistological staining for CD68, lysozyme, CD1a, S-100 protein, CD21, and CD35 is recommended for the differential diagnosis of HS. HS expressed CD68 and lysozyme, but negative for Langerhans (CD1a) and dendritic cell markers (CD21 and CD35) with focal reactivity for S-100 protein [4]. Recently, CD163 has been recognized as a new macrophage-related differentiation marker, which is more specific than the conventional histiocyte-related molecules [2, 3, 5]. HS is a rare neoplasm and, by our search, CD163 staining was evaluated in 28 cases as summarized in Table 1 [3, 5–20]. There are several reports of HS patients arising from other neoplasms, such as acute lymphoblastic leukemia, chronic lymphocytic leukemia, malignant lymphoma, and germ cell tumor [13–16, 20–22]. Our patient had been pointed out the right hilar lymphadenopathy 13 years before the diagnosis of HS. Although the etiology of lymphadenopathy was equivocal, it is possible that HS can arise from any lymphoproliferative disease.

In this case, there were two populations of phenotypically distinct tumor cells in the left neck lymph node and stomach: (A) lysozyme-positive round cells with no expression of CD163 and (B) CD163-positive cells, which were rich in cytoplasm or spindle shaped with no expression of lysozyme. Since macrophages in the normal lymph node have abundant cytoplasm and are positive for CD163 (Fig. 1a-4) [2], many of CD163-positive cells in the cervical lymph node were likely tissue resident or reactive macrophages. Activated macrophages are CD163-positive [23]; however, vast majority of oval and relatively small population (A) were positive for lysozyme but negative for CD163. Together with the atypical morphology, population (A) is likely the main HS cells in this stage. On the other hand, the tumor cells derived from the right hilar lymph node and other organs during autopsy were spindle-shaped and diffusely positive for CD163 but negative for lysozyme, which was similar to a HS case reported by Alexiev et al. [10]. Considering the clinical finding that the latter lesions were less sensitive to treatment, the expression of CD163 in HS could be a biomarker correlated with chemoradio resistance. Interestingly, Yoshida et al. [6] have reported a case of HS with only sporadic staining for CD163, and this case was quite sensitive to chemotherapy.

CD163 distributes to skin histiocytes, Kupffer cells, splenic red pulp macrophages, and some thymus macrophages [24, 25]. This antigen is a member of the scavenger receptor cysteine-rich family class B restricted to the macrophage/monocyte lineage [25, 26]. The function of CD163 molecule was first identified as a scavenger receptor for haptoglobin–hemoglobin complex [27, 28]. Because CD163 expression is induced by interleukin (IL)-6, IL-10, and glucocorticoids, and is down-regulated by lipopolysaccharide and interferon-γ, it is thought to be one

Table 1 Reported cases of HS with CD163 staining

	Reference	Age/sex	Location	CD163	CD68	lys	Ki-67 (%)
1.	Current case	73/M	Cervical LN				
			Population (A)	–	+	+	19
			Population (B)	+	+	–	0
			Hilar LN (spindle-shaped)	+	+	–	0
2.	Vos et al. [3]	72/M	Palatal nodule	+	+	wk+	5
3.	Vos et al. [3]	69/M	Peripancreatic mass, skin	+	+	+	5
4.	Vos et al. [3]	20/F	Colon, BM	+	+	+	15
5.	Vos et al. [3]	55/F	Colon	+	+	+	0–10
6.	Vos et al. [3]	73/F	Inguinal LN	+	+	wk+	15
7.	Mikami et al. [5]	69/M	Skin, BM	+	+	+	ND
8.	Yoshida et al. [6]	56/M	BM	F	+	+	ND
9.	Huang et al. [7]	27/F	Ovary, appendix, ileum	+	+	+	ND
10.	Cao et al. [8]	53/F	CNS, mediastinum	+	+	ND	20
11.	Abidi et al. [9]	48/F	Systemic mass	+	+	ND	ND
12.	Alexiev et al. [10]	41/M	Head, neck	+	+	+	70
13.	Oka et al. [11]	58/F	Spleen	+	+	+	ND
14.	Kobayashi et al. [12]	82/F	Spleen	+	+	ND	33
15.	Feldman et al. [13]	62/M	Pelvis	+	+	+	ND
16.	Feldman et al. [13]	30/F	Cervical LN	–	+	–	ND
17.	Feldman et al. [13]	60/M	Cervical LN	+	+	+	ND
18.	Feldman et al. [13]	48/F	Thigh mass	+	+	+	ND
19.	Feldman et al. [13]	62/M	Axillary mass	ND	+	+	ND
20.	Feldman et al. [13]	58/M	Tongue, cervical LN	+	+	F	ND
21.	Feldman et al. [13]	67/M	Skin	+	+	+	ND
22.	McClure et al. [14]	25/M	Spleen, skin	+	+	wk+	ND
23.	Zhang et al. [15]	50/M	Hipbone mass	+	+	+	ND
24.	Shinoda et al. [16]	24/M	Spleen	+	+	ND	ND
25.	Yu et al. [17]	69/M	Thyroid grand	+	+	+	31
26.	Yang et al. [18]	80/M	Lung mass	+	+	+	30–40
27.	Venkataraman et al. [19]	13/M	Para-abdominal LN	+	+	–	20–40
28.	Mori et al. [20]	70/M	Peri-vertebral mass, BM	+	+	+	ND

lys lysozyme, *wk+* weak, *F* focal, *ND* not done, *BM* bone marrow, *LN* lymph node

of the molecules associated with anti-inflammatory macrophages phenotype [24, 25]. Recent report demonstrated that CD163 can function as a macrophage receptor for Gram-positive and negative bacteria, and a previously identified cell-binding motif in the second scavenger domain of CD163 was sufficient to mediate this binding [29]. In the presence of a bacterial infection, CD163 on resident tissue macrophages likely acts as an innate immune sensor and inducer of local inflammation under normal condition. Interestingly, CD163-positive monocytes are shown to inhibit proliferation of CD4-positive T cells in co-culture [30], and a soluble form of CD163 also inhibits T cell proliferation in vitro [31, 32]. It is possible that the tumor cells escape from anti-tumor immunity of cytotoxic T cells by high expression of CD163, resulting in the refractory state and the poor prognosis of HS.

CD163 has been recognized to be important for the diagnosis of HS, but it requires attention that there could be CD163-negative tumor cells in HS, which may remain reactive for the treatment.

References

1. Rappaport H. Tumors of the hematopoietic system. Washington, DC: US Armed Forces Institute of Pathology; 1966.
2. Lau SK, Chu PG, Weiss LM. CD163: a specific marker of macrophages in paraffin-embedded tissue samples. Am J Clin Pathol. 2004;122:794–801.
3. Vos JA, Abbondanzo SL, Barekman CL, Andriko JW, Miettinen M, Aguilera NS. Histiocytic sarcoma: a study of five cases including the histiocyte marker CD163. Mod Pathol. 2005;18:693–704.

4. Pileri SA, Grogan TM, Harris NL, et al. Tumours of histiocytes and accessory dendritic cells: an immunohistochemical approach to classification from the International Lymphoma Study Group based on 61 cases. Histopathology. 2002;41:1–29.
5. Mikami M, Sadahira Y, Suetsugu Y, Wada H, Sugihara T. Monocyte/macrophage-specific marker CD163+ histiocytic sarcoma: case report with clinical, morphologic, immunohistochemical, and molecular genetic studies. Int J Hematol. 2004;80:365–9.
6. Yoshida C, Takeuchi M. Histiocytic sarcoma: identification of its histiocytic origin using immunohistochemistry. Intern Med. 2008;47:165–9.
7. Huang SC, Chang CL, Huang CH, Chang CC. Histiocytic sarcoma—a case with evenly distributed multinucleated giant cells. Pathol Res Pract. 2007;203:683–9.
8. Cao M, Eshoa C, Schultz C, Black J, Zu Y, Chang CC. Primary central nervous system histiocytic sarcoma with relapse to mediastinum: a case report and review of the literature. Arch Pathol Lab Med. 2007;131:301–5.
9. Abidi MH, Tove I, Ibrahim RB, Maria D, Peres E. Thalidomide for the treatment of histiocytic sarcoma after hematopoietic stem cell transplant. Am J Hematol. 2007;82:932–3.
10. Alexiev BA, Sailey CJ, McClure SA, Ord RA, Zhao XF, Papadimitriou JC. Primary histiocytic sarcoma arising in the head and neck with predominant spindle cell component. Diagn Pathol. 2007;2:7.
11. Oka K, Nakamine H, Maeda K, et al. Primary histiocytic sarcoma of the spleen associated with hemophagocytosis. Int J Hematol. 2008;87:405–9.
12. Kobayashi S, Kimura F, Hama Y, et al. Histiocytic sarcoma of the spleen: case report of asymptomatic onset of thrombocytopenia and complex imaging features. Int J Hematol. 2008;87:83–7.
13. Feldman AL, Arber DA, Pittaluga S, et al. Clonally related follicular lymphomas and histiocytic/dendritic cell sarcomas: evidence for transdifferentiation of the follicular lymphoma clone. Blood. 2008;111:5433–9.
14. McClure R, Khoury J, Feldman A, Ketterling R. Clonal relationship between precursor B-cell acute lymphoblastic leukemia and histiocytic sarcoma: a case report and discussion in the context of similar cases. Leuk Res. 2009;34:e71–3.
15. Zhang D, McGuirk J, Ganguly S, Persons DL. Histiocytic/dendritic cell sarcoma arising from follicular lymphoma involving the bone: a case report and review of literature. Int J Hematol. 2009;89:529–32.
16. Shinoda H, Yoshida A, Teruya-Feldstein J. Malignant histiocytoses/disseminated histiocytic sarcoma with hemophagocytic syndrome in a patient with mediastinal germ cell tumor. Appl Immunohistochem Mol Morphol. 2009;17:338–44.
17. Yu L, Yang SJ. A case of primary histiocytic sarcoma arising from thyroid gland. Pathol Oncol Res. 2010;16:27–132.
18. Yang GC, Besanceney CE, Tam W. Histiocytic sarcoma with interdigitating dendritic cell differentiation: a case report with fine needle aspiration cytology and review of literature. Diagn Cytopathol. 2010;38:351–6.
19. Venkataraman G, McClain KL, Pittaluga S, Rao VK, Jaffe ES. Development of disseminated histiocytic sarcoma in a patient with autoimmune lymphoproliferative syndrome and associated Rosai–Dorfman disease. Am J Surg Pathol. 2010;34:589–94.
20. Mori M, Matsushita A, Takiuchi Y, et al. Histiocytic sarcoma and underlying chronic myelomonocytic leukemia: a proposal for the developmental classification of histiocytic sarcoma. Int J Hematol. 2010;92:168–73.
21. deMent SH. Association between mediastinal germ cell tumors and hematologic malignancies: an update. Hum Pathol. 1990;21:699–703.
22. Ikdahl T, Josefsen D, Jakobsen E, Delabie J, Fossa SD. Concurrent mediastinal germ-cell tumour and haematological malignancy: case report and short review of literature. Acta Oncol. 2008;47:466–9.
23. Nishiwaki S, Terakura S, Ito M, et al. Impact of macrophage infiltration of skin lesions on survival after allogeneic stem cell transplantation: a clue to refractory graft-versus-host disease. Blood. 2009;114:3113–6.
24. Polfliet MM, Fabriek BO, Daniels WP, Dijkstra CD, van den Berg TK. The rat macrophage scavenger receptor CD163: expression, regulation and role in inflammatory mediator production. Immunobiology. 2006;211:419–25.
25. Hogger P, Dreier J, Droste A, Buck F, Sorg C. Identification of the integral membrane protein RM3/1 on human monocytes as a glucocorticoid-inducible member of the scavenger receptor cysteine-rich family (CD163). J Immunol. 1998;161:1883–90.
26. Law SK, Micklem KJ, Shaw JM, et al. A new macrophage differentiation antigen which is a member of the scavenger receptor superfamily. Eur J Immunol. 1993;23:2320–5.
27. Kristiansen M, Graversen JH, Jacobsen C, et al. Identification of the haemoglobin scavenger receptor. Nature. 2001;409:198–201.
28. Fabriek BO, Dijkstra CD, van den Berg TK. The macrophage scavenger receptor CD163. Immunobiology. 2005;210:153–60.
29. Fabriek BO, van Bruggen R, Deng DM, et al. The macrophage scavenger receptor CD163 functions as an innate immune sensor for bacteria. Blood. 2009;113:887–92.
30. Schebesch C, Kodelja V, Muller C, et al. Alternatively activated macrophages actively inhibit proliferation of peripheral blood lymphocytes and CD4+ T cells in vitro. Immunology. 1997;92:478–86.
31. Hogger P, Sorg C. Soluble CD163 inhibits phorbol ester-induced lymphocyte proliferation. Biochem Biophys Res Commun. 2001;288:841–3.
32. Frings W, Dreier J, Sorg C. Only the soluble form of the scavenger receptor CD163 acts inhibitory on phorbol ester-activated T-lymphocytes, whereas membrane-bound protein has no effect. FEBS Lett. 2002;526:93–6.

Kobe J. Med. Sci., Vol. 56, No. 2, pp. E38-E49, 2010

Vitamin K2-derived Compounds Induce Growth Inhibition in Radioresistant Cancer Cells

HELFI AMALIA[1], RYOHEI SASAKI[1], YOKO SUZUKI[1], YUSUKE DEMIZU[2], TOSHINORI BITO[3], HIDEKI NISHIMURA[1], YOSHIAKI OKAMOTO[1], KENJI YOSHIDA[1], DAISUKE MIYAWAKI[1], TETSUYA KAWABE[1], YOSHIYUKI MIZUSHINA[4,5], and KAZURO SUGIMURA[1]

[1] *Divisions of Radiation Oncology, and [3]of Dermatology, Kobe University Graduate School of Medicine, 7-5-2 Kusunokicho Chuouku Kobe City, Hyogo 650-0017, Japan*

[2] *Department of Radiology, Hyogo Ion Beam Medical Center, Tatsuno City, Hyogo, Japan*

[4] *Laboratory of Food & Nutritional Sciences, Department of Nutritional Science, Kobe-Gakuin University, Nishi-ku, Kobe, Hyogo, Japan*

[5] *Cooperative Research Center of Life Sciences, Kobe-Gakuin University, Chuo-ku, Kobe, Hyogo, Japan*

Received 7 January 2010/ Accepted 18 January 2010

Key Words: Radioresistance, Vitamin K, NF-kappa B, Reactive oxygen species, Cancer

A strategy to overcome radioresistance in cancer treatment has been expected. To evaluate the strategy, appropriate experimental models are needed. Radioresistant tumour models were originally established from human colon cancer cells, and we evaluated their molecular basis. Next, the growth inhibitory effects of newly synthesized vitamin K2 (VK2)-related compounds were tested. Here, we showed that these novel compounds have growth inhibitory effects not only on cancer cells of various origins, but also on radioresistant cells, through the generation of reactive oxygen species (ROS).

Human colon, lung, and breast cancer cell lines were used for testing the growth inhibitory activities of several chemical compounds. Radioresistant tumour models were established by fractionated radiation exposure. Irradiated cells were selected by a single cell cloning method, and their sensitivity to ionizing radiation was evaluated by a colony-forming assay. The VK2 derivatives (named MQ-1, MQ-2, and MQ-3) were chemically synthesized. To evaluate the generation of ROS, flow cytometer analyses were performed.

A radioresistant tumour model was established from the HCT116 human colon cancer cell line. The radioresistant cells from HCT116 also showed resistance to cisplatin. In the radioresistant cells, NF-κB was highly activated. MQ-1, MQ-2, and MQ-3 showed greater growth inhibitory activities than VK2 not only in various cancer cells but also in radioresistant cells through the generation of ROS.

In conclusion, a radioresistant tumour model was originally established from colon cancer cell lines through NF-κB activation, and it could be a useful tool for evaluating anti-tumour agents. Newly synthesized VK2 derivatives (MQ-1, MQ-2 and MQ-3) seemed to be potential anti-tumour agents in various cancers and radioresistant cancers. The efficacy of those compounds was related to the generation of ROS. These findings together might pave the way for the treatment of radioresistant or recurrent cancers.

Phone: 81-78-382-6104 Fax: 81-78-382-6129 E-mail: rsasaki@med.kobe-u.ac.jp

Vitamin K is a generic term for certain derivatives of 2-methyl-1,4 naphtoquinone, which was discovered in 1929 by Henrik Dam as a fat-soluble anti-hemorrhagic agent (5). There are two naturally occurring forms of vitamin K. Phylloquinone, also known as vitamin K1 (VK1), is found in higher plants. The menaquinone series are collectively referred to as vitamin K2 (VK2) and are synthesized by bacteria. Menadione (vitamin K3: VK3) is a synthetic derivative of beta-naphthalene (4-5, 12-13, 19, 28). Compounds with a quinone structure are reported to play a prominent role in cancer chemotherapy (5). VK2 is known to have a marginally active growth inhibitory activity, whereas VK3 is a distinct inhibitor of cell growth, both in vitro and in vivo (9, 12, 14, 24, 38-41, 44-45).

Although several reports suggested that vitamin Ks might induce cell cycle arrest or cell death, their mechanisms of growth inhibition remain largely undetermined (5, 12, 19). There are several reports concerning vitamin K and its analogues showing that the growth inhibitory activity decreased with increasing side-chain length (28). VK3 has the shortest side-chain and is reported to show a distinct cytotoxicity that is equal or superior to a number of standard antitumor agents. However, VK3 induced severe adverse effects in vivo, including haemolytic anaemia; consequently, VK3 was left out of mainstay cancer treatment regimens (5-6, 22, 25-26). VK2 is less toxic and has been reported to induce apoptosis or autophagy in certain cancer cell lines (9, 12, 14, 24, 38-41, 44-45). Although VK3 was believed to combat oxidative stress via redox cycling of the quinone to produce reactive oxygen species (12, 19, 38), it has not been clarified that the cytotoxic action of VK2 was due to the same mechanism as that of VK3.

In our previous report, we demonstrated that VK3 showed excellent cytotoxicity through the generation of reactive oxygen species (ROS) by affecting mitochondria (36). In the study, VK2 showed weaker but apparent cytotoxicity in certain cell lines, and Shibayama also reported similar results in different cancer cell lines (39). We further hypothesized that compounds that shortened the side chain of VK2 might confer both advantages of the growth inhibitory effect of VK3 against cancerous cells and a lesser toxicity of VK2 to normal cells and that those VK-2 related compounds might function as anti-tumour agents. Compounds were originally generated from VK2, and we tested those growth inhibitory activities. Here, we showed that those novel compounds have growth inhibitory effects not only on cancer cells of various origins, but also on radioresistant clones, through the generation of ROS.

MATERIALS AND METHODS

1. Cell lines and chemicals

HCT116 human colon carcinoma cell lines with wild-type p53 (HCT116 p53+/+) and their isogenic derivatives that lack p53 (HCT116 p53−/−) were a kind gift from Dr. Bert Vogelstein (Johns Hopkins University, Baltimore). The cells were maintained in McCoy's 5A medium containing 10% foetal bovine serum (FBS) or in McCoy's 5A-based enriched medium with 10% FBS, 2 mM sodium pyruvate, 50 μg/ml uridine added to the normal medium at 37°C with 5% CO_2. H1299 and MCF-7 were obtained from ATCC and cultured in RPMI-1640 and DMEM medium. VK1, VK2, VK3, doxorubicine, gemcitabine, taxol, TNF-α and N-acetylcysteine (NAC) were purchased from Sigma (St. Louis, MO, USA). Dihydroethidine (HE) and 5-carboxy-2',7'dichlorodihydrofluorescein diacetate (c-DCF) were obtained from Molecular Probes (Eugene, OR, USA). Aminophenyl fluorescein (APF) was purchased from Sekisui Medical (Tokyo, Japan) (37). All other reagents were purchased from Nakalai Tesque Ltd. (Kyoto, Japan)

2. Preparation of vitamin K2 derivatives (MQ-1, MQ-2, MQ-3)

The VK2 derivatives (named MQ-1, MQ-2, and MQ-3) were chemically synthesized according to the procedure reported by Mayer and Isler with minor modifications (23). The structures of these compounds were confirmed by comparison of the spectral data with those reported. All reactions were monitored by thin liquid chromatography (TLC), which was carried out on Silica Gel 60 F_{254} plates (Merck, Germany). Flash chromatography separations were performed on PSQ 100B (Fuji Silysia Co., Ltd., Japan). ^{1}H and ^{13}C NMR spectra were recorded on a JEOL 270 MHz spectrometer (EX-270W), using $CDCl_3$ (with TMS for ^{1}H NMR and chloroform-d for ^{13}C NMR as the internal reference) solution unless otherwise noted. Chemical shifts were expressed in d (ppm) relative to Me_4Si or residual solvent resonance, and coupling constants (J) were expressed in Hz. Melting points were determined with a Yanaco MP-3S and were uncorrected. Infrared (IR) spectra were recorded on a Jasco FT/IR-410 spectrometer using NaCl (neat) or KBr pellets (solid) and were reported as wavenumbers (cm^{-1}). Mass spectra (MS) were obtained on an Applied Biosystems mass spectrometer (APIQSTAR pulsar i) under high-resolution conditions, using polyethylene glycol as an internal standard.

3. Analyses of cellular superoxide, hydrogen peroxide, and the hydroxyl radical

Cellular superoxide and hydrogen peroxide were measured by flow cytometer analyses using HE and c-DCF (33, 36). HE was dissolved in DMSO (100 mg/ml stock) and further diluted with PBS at 1:10,000. The diluted dye was added to the cell culture at a final concentration of 50 ng/ml and incubated at 37°C during the last 60 min. c-DCF was also dissolved in DMSO (20 mM stock) and used for staining at 50 μM at 37°C for 60 min. Cellular hydroxyl radical were also measured by flow cytometer according to the manufacturer's instructions (37).

4. Electrophoretic mobility shift assay (EMSA) for NF-κB

Nuclear extracts were prepared, and EMSAs were performed essentially as described previously (2). Binding reaction mixtures (20 μl) containing 5 μg protein of nuclear extract, 2 μg poly(dI-dC) (Pharmacia, Sweden), ^{32}P-labeled NF-κB p65 probe (Santa Cruz, CA, USA), 50 mM NaCl, 2 mM $MgCl_2$, 0.2 mM Na_2EDTA, 1 mM dithiothreitol (DTT), 10% (v/v) glycerol and 4 mM Tris-HCl (pH 7.9) were incubated for 30 min at room temperature. Proteins were separated by electrophoresis in a native 6% polyacrylamide gel using a Tris-borate-EDTA running buffer (12.5 mM Tris-borate containing 0.25 mM Na_2EDTA, pH 8.0) followed by autoradiography.

5. Western blot analysis

Total cell lysates were prepared and separated by electrophoresis on 8-12% SDS-PAGE, essentially as described previously (1). Antibodies for NF-κB p65 (Santa Cruz, CA, USA) and β-actin (Sigma) were used. The primary antibodies were diluted at 1:1,000-1:5,000 and detected using appropriate horseradish peroxidase-conjugated secondary antibodies, followed by detection with a SuperSignal enhanced chemiluminescence kit (Pierce, Rockford, IL, USA). Immune complexes were detected by chemiluminescence and then by fluorescence using a LAS3000 mini lumino image-analyzer (FUJI FILM, Tokyo, Japan). The density of each band was quantitatively evaluated using Multi Gauge Version 3.0 (FUJI FILM).

6. Cytotoxicity (MTT) assay and long-term survival (colony-forming) assay

Cytotoxicity was determined by a 3-(4,5-dimethyl thiazol-2)-2,5-diphenyltetrazolium bromide (MTT) assay (72 h), as described previously (36). For a longer-term survival analysis, a colony-forming assay was performed. Cells were incubated for 10-14 days. Fixation and staining were according to previously described methods (8, 34-35).

RESULTS

1. Establishment of radioresistant cells from human colon cancer cell lines.

The first objective of our experimental protocol was to establish an in vitro model that would mimic our clinical observation in terms of the variable response to ionizing radiation. We used two kinds of HCT116 cells: one that is p53 wild type (HCT116 p53+/+) and the other that is p53-deficient (HCT116 p53−/−). After exposure to fractionated irradiation, surviving cells were tested as to whether they could grow by themselves and form a colony (single cell cloning method). Several colonies were isolated as candidates for radioresistant clones. As a result, irradiated clones HCT116 p53+/+ were more resistant than the parental cells, whereas irradiated clones from HCT116 p53−/− showed similar sensitivities to those of their parental cells (Figure 1). Next, the sensitivities of those radioresistant clones to anti-tumour agents were tested (Table I). As for cisplatin, resistant clones of HCT116 p53+/+ showed more than 10-fold greater resistance than their parental cells and resistant clones of HCT116 p53−/− showed 3-fold greater resistance, whereas those clones had similar sensitivities to doxorubicin, gemcitabine, and taxol as their parental cells.

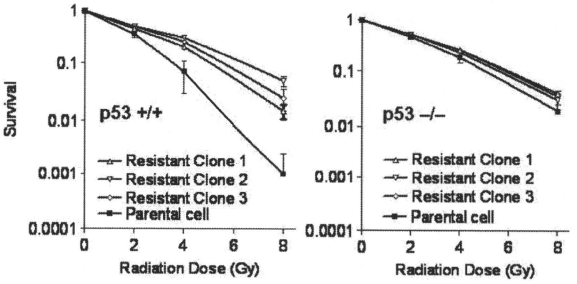

Figure 1. Establishment of radioresistant clones from HCT116 human colon cancer cells. Error bars from 3 independent experiments.

Table I. Comparison of drug sensitivities between HCT116 and radioresistant cells.

	IC_{50} (μM)			
	HCT116 p53+/+		HCT116 p53−/−	
	WT	Resistant	KO	Resistant
Doxorubicine	0.05	0.15	0.12	0.15
Cisplatine	1.5	18	3.5	10.5
Gemcitabine	0.008	0.012	0.015	0.015
Taxol	0.005	0.015	0.007	0.008

Footnotes: WT=wild type, KO=knockout

2. NF-κB activation in radioresistant cells

Characteristics of HCT116 parental cells and their radioresistant clones were investigated, especially in terms of the relationship to NF-κB activation. First, the binding activity of parental cells of HCT116 p53+/+ and of HCT116 p53−/− and their resistant clones were tested. Resistant clones of HC116 p53+/+ showed higher binding activity compared to the parental cells (Figure 2A). In contrast, the parental HCT116 p53−/− and their resistant clones had slightly higher binding than the HC116 p53+/+ cells but similar to HC116 p53+/+ resistant clones. Next, responses to ionizing radiation in HCT116 p53+/+ parental and resistant clones were tested by western blotting (Figure 2B). The amount of NF-κB increased in response to the irradiation in the parental cells. The amounts of activated NF-κB in HCT116 p53+/+ resistant clones were higher than those in the parental cells (Figure 2B).

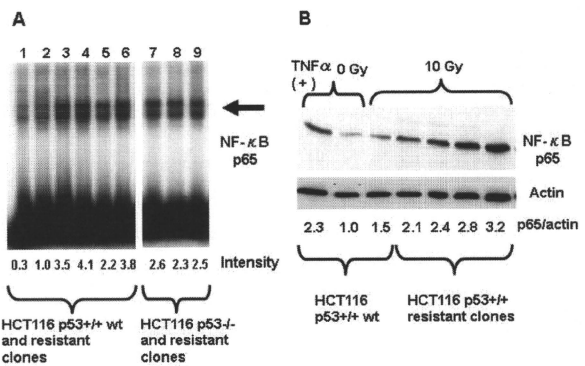

Figure 2. Radioresistance acquired through NF-κB activation. A. EMSA assay for NF-κB (Lane 1:cold probe, L2: HC116 p53+/+, L3-L6: HC116 p53+/+ resistant clones, L7: HCT116 p53−/−, L8-L9: HCT116 p53−/− resistant clones, B. Western blotting analysis for NF-κB with or without 10 Gy of irradiation (TNFα for positive control). Both EMSA and western blotting assays were performed at least twice and a representative datum was shown.

3. Generation of vitamin K2 derivatives

Three VK2 derivatives were chemically synthesized according to the procedure shown in the Methods and Materials. Three derivatives were established, named MQ-1, MQ-2, and MQ-3, which all shared a methylated naphthoquinone ring structure and were varied in the isoprenoid side chains. The molecular weights of MQ-1, MQ-2, and MQ-3 were 240.3, 308.4, and 376.5, respectively (Figure 3).

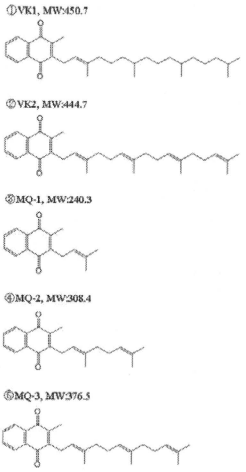

Figure 3. Structures and molecular weights of vitamin K1, K2, and VK2 derivatives (MQ-1, MQ-2, and MQ-3).

4. Growth inhibitory effects of MQ-1, MQ-2, and MQ-3, in various cancer cells

Growth inhibitory activities of MQ-1, MQ-2, and MQ-3 were assessed in various human cancer cells in comparison with that of VK2. All of those derivatives obtained greater growth inhibitory activities than VK2 in HCT116 human colon cancer cells, H1299 human lung cancer cells, and MCF-7 human breast cancer cells (Figure 4); therefore, the length of isoprenoid residue of VK2 must be important for the activity. Surprisingly, radioresistant clones of HCT116 showed similar growth inhibitory effects to those derivatives as HCT116 wt did (Table II). This result suggested that those derivatives could be promising compounds against radioresistant tumours. In addition, those growth inhibitory activities of MQ-1, MQ-2, and MQ-3 to HCT116, H1299, and MCF-7 cells were much weaker than that of VK3 (data not shown). Therefore, those derivatives showed intermediate growth inhibitory activities between those of VK2 and VK3.

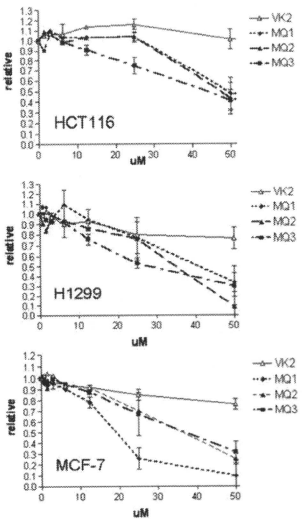

Figure 4. Comparison of growth activities between VK2 and VK2 derivatives in various cancer cells. Error bars from 3 independent experiments.

Table II. Comparison of the growth inhibitory activities of vitamin K1, K2, and VK2 derivatives.

		IC50 (μM)				
Cell Type	Tissue origin	VK1	VK2	MQ1	MQ2	MQ3
HCT116 wt	Colon	>100	>100	50	46	42
HCT116 Resistant clone	Colon	>100	>100	52	35	40
H1299	Lung	>100	>100	40	33	29
MCF-7	Breast	>100	>100	20	38	40

5. Reactive oxygen species (ROS) generation by vitamin K2 derivatives in HCT116 cells

Because the mechanisms of cytotoxicity of VK3 were determined to occur through reactive oxygen species generation in the previous study (36), the actions of MQ-1, MQ-2, and MQ-3 for free radical generation were investigated. These compounds induced greater amounts of superoxide, hydrogen peroxide, and hydroxyl radicals compared to VK2 in HCT116 cells (Figure 5). Next, free radical generation was tested in radioresistant clones of HCT116. The induction of superoxide, hydrogen peroxide, and hydroxyl radicals by

superoxide, hydrogen peroxide, and hydroxyl radical in the radioresistant clones was almost similar to that in HCT116 cells (Figure 5). To clarify whether the free radical generation affected the cytotoxicities of MQ-1, MQ-2, and MQ-3, a ROS scavenger, N-acetylcysteine (NAC), was tested. With 5 mM of NAC administration, the IC_{50} of those VK2 derivatives in HCT116 cells were decreased (50 μM by MQ-1 only versus 100 μM by MQ-1 and NAC; 46 μM by MQ-2 only versus 85 μM by MQ-2 and NAC; 42 μM by MQ-3 only versus 56 μM by MQ-3 and NAC). These data indicated that the cytotoxicities of VK2 derivatives proceeded through the generation of ROS.

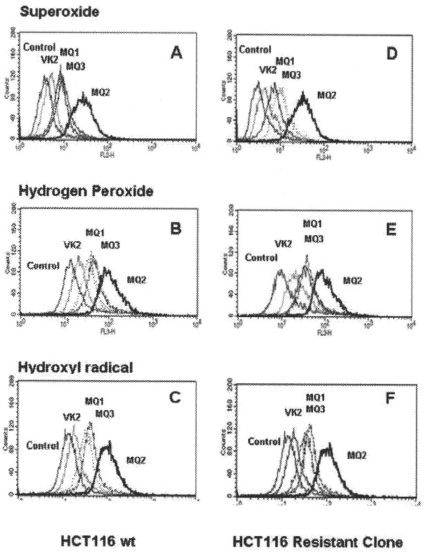

Figure 5. Generation of reactive oxygen species induced by VK2 and VK2 derivatives in HCT116 and radioresistant cells.

DISCUSSION

Although many factors have been reported to be candidates for determining cellular radioresistance, how cancer cells obtain radioresistance is largely unknown (29). The p53 protein has been intensively assessed in this regard. It has been reported that p53 mutations in several cancer cells were associated with increased radioresistance because of the failure to induce apoptosis following radiation (3, 7, 21, 35). Our data using the human colon cancer cell HCT116 and the counterpart of p53-deficient HCT116 cells strongly supported the notion that p53 was a major determinant of radioresistance. However, in the process of establishing radioresistant models, only wild-type HCT116 became resistant to ionizing radiation, and normal p53 function was retained. Therefore, we tested an alternative major

determinant of radioresistance, NF-κB. NF-κB activity has been widely reported to be linked to chemoresistance in multiple tumours (31), as well as with radioresistance in experimental models (17-18, 20, 27, 42-43). We first reported in the clinical setting that NF-κB was the strongest factor predicting radioresistance in early stage laryngeal squamous cell carcinomas and that more than 90% of recurrent laryngeal cancer after curative radiotherapy showed highly activated NF-κB (46). In this study of colon adenocarcinoma, NF-κB was increased in the process of obtaining radioresistance in wild-type HCT116 cells and was already activated in p53-deficient cells. Although both p53 and NF-κB are important transcriptional factors for various genes (10, 18, 27, 29), NF-κB might affect the acquisition of radioresistance in the situation where p53 is normal.

Several investigators reported that vitamin K analogues have growth inhibitory effects, especially on hepatoma cells and hematopoietic or myeloma cells (12, 24, 28, 41, 44). Carr and co-workers investigated the growth inhibitory effects of their originally synthesized vitamin K-related compounds (28). Although they synthesized several vitamin K analogues of side chains with a sulphur (thioether) or oxygen atom (*O*-ether) at the site of attachment of the side chain to the ring, the potency to induce apoptosis in hepatoma cells was correlated with the decreasing length of the side chain. In contrast, Shibayama and co-workers reported that VK2 induced apoptosis through the generation of ROS in ovarian cancer cells (39). Ozaki and co-workers reported that vitamin K2 inhibited hepatoma cell proliferation by regulating cyclin D1 expression through the inhibition of NF-κB activation (31). In this study, we originally synthesized a VK analogue from VK2, and those compounds had cytotoxic effects not only in various cancer cells but also in radioresistant cells. These seemed to be novel findings, and these observations might pave the way in the novel strategy against recurrent cancer after radiotherapy.

Although acquired tumour radioresistance during radiotherapy is believed to be due to tumour repopulation (15), the exact molecular mechanisms underlying the radioadaptive response are largely unknown. NF-κB is reported to play a central role in the response through multiple pathways (16). In addition, Orlowski demonstrated that elevated basal NF-κB activity in certain cancers has been linked with tumour resistance to chemotherapy and radiation (30), and the established radioresistant cells in this study were consistent with this tendency. Although not all experiments show an enhanced radiosensitivity due to NF-κB inhibition (11, 32), NF-κB seems to be a key molecule to overcome radioresistance. It seems quite promising for a future strategy that VK-2 derivatives showed a growth inhibitory effect in radioresistant clones.

In conclusion, a radioresistant tumour model was originally established from colon cancer cell lines through NF-κB activation, and it could be a useful tool for evaluating anti-tumour agents. Newly synthesized VK2 derivatives (MQ-1, MQ-2 and MQ-3) seemed to be potential anti-tumour agents in various cancers and radioresistant cancers. The efficacy of those compounds was related to the generation of reactive oxygen species. These findings together might pave the way for the treatment of radioresistant or recurrent cancers.

ACKNOWLEDGEMENTS

This work was supported by Grants-in-aid 18209040, 19591458, 21591609, 20890127, 21791195 for Scientific Research, MEXT (Ministry of Education, Culture, Sports, Science and Technology, Japan) (Syogo Yamada, Tohoku, Japan and Ryohei Sasaki). The authors acknowledge Dr. Kouji Kuramochi, Mr. Ryo Mizutani, Mr. Kazuyuki Nishio, and Dr. Kazunori Tsubaki of Kyoto Prefectural University (Kyoto, Japan) for the synthesis of the vitamin K2 derivatives (MQ-1, MQ-2, and MQ-3).

REFERENCES

1. **Achanta, G., Sasaki, R., Feng, L., Carew, J.S., Lu, W., Pelicano, H., Keating, M.J., Huang, P.** 2005. Novel role of p53 in maintaining mitochondrial genetic stability through interaction with DNA Pol gamma. EMBO J **24:**3482-92.
2. **Bito, T., Roy, S., Sen, C.K., Shirakawa, T., Gotoh, A., Ueda, M., Ichihashi, M., Packer, L.** 2002. Flavonoids differentially regulate IFN gamma-induced ICAM-1 expression in human keratinocytes: molecular mechanisms of action. FEBS Lett **520:**145-52.
3. **Bristow, R.G., Benchimol, S., Hill, R.P.** 1996. The p53 gene as a modifier of intrinsic radiosensitivity: implications for radiotherapy. Radiother Oncol **40:**197-223.
4. **Carr, B.I., Wang, Z., Kar, and S.K.** 2002. vitamins, PTP antagonism, and cell growth arrest. J Cell Physiol **193:**263-74.
5. **Chlebowski, R.T., Akman, S.A., Block, J.B.** 1985. Vitamin K in the treatment of cancer. Cancer Treat Reviews **12:**49-63.
6. **Cojocel, C., Novotny, L., Vachalkova, A.** 2006. Mutagenic and carcinogenic potential of menadione. Neoplasma **53:**316-23.
7. **Dahm-Daphi, J.** 2000. p53: biology and role for cellular radiosensitivity. Strahlenther Onkol **176:**278-85.
8. **Demizu, Y., Kagawa, K., Ejima, Y., Nishimura, H., Sasaki, R., Soejima, T., Yanou, T., Shimizu, M., Furusawa, Y., Hishikawa, Y., Sugimura, K.** 2004. Cell biological basis for combination radiotherapy using heavy-ion beams and high-energy X-rays. Radiother Oncol **71:**207-11.
9. **Enomoto, M., Tsuchida, A., Miyazawa, K., Yokoyama, T., Kawakita, H., Tokita, H., Naito, M., Itoh, M., Ohyashiki, K., Aoki, T.** 2007. Vitamin K2-induced cell growth inhibition via autophagy formation in cholangiocellular carcinoma cell lines. Int J Mol Med **20:**801-8.
10. **Eschrich, S.A., Pramana, J., Zhang, H., Zhao, H., Boulware, D., Lee, J.H., Bloom, G., Rocha-Lima, C., Kelley, S., Calvin, D.P., Yeatman, T.J., Begg, A.C., Torres-Roca, J.F.** 2009. A gene expression model of intrinsic tumor radiosensitivity: prediction of response and prognosis after chemoradiation. Int J Radiat Oncol Biol Phys **75:**489-96.
11. **Flynn, Jr. V., Ramanitharan, A., Moparty, K., Davis, R., Sikka, S., Agrawal, K.C., Abdel-Mageed, A.B.** 2003. Adenovirus-mediated inhibition of NF-κB confers chemo-sensitization and apoptosis in prostate cancer cells. Int J Oncol **23:**317-23.
12. **Hitomi, M., Yokoyama, F., Kita, Y., Nonomura, T., Masaki, T., Yoshiji, H., Inoue, H., Kinekawa, F., Kurokohchi, K., Uchida, N., Watanabe, S., Kuriyama, S.** 2005. Antitumor effects of vitamins K1, K2 and K3 on hepatocellular carcinoma in vitro and in vivo. Int J Oncol **26:**713-20.
13. **Kar, S., and Carr, B.I.** 2000. Growth inhibition and protein tyrosine phosphorylation in MCF-7 breast cancer cells by a novel K vitamin. J Cell Physiol **185:**386-93.
14. **Kawakita, H., Tsuchida, A., Miyazawa, K., Naito, M., Shigoka, M., Kyo, B., Enomoto, M., Wada, T., Katsumata, K., Ohyashiki, K., Itoh, M., Tomoda, A., Aoki, T.** 2009. Growth inhibitory effects of vitamin K2 on colon cancer cell lines via different types of cell death including autophagy and apoptosis. Int J Mol Med **23:**709-16.
15. **Kazi, M.A., Jian, J.L.** 2008. NF-κB-mediated adaptive resistance to ionizing radiation. Free Radic Biol Med **44:**1-13.
16. **Kim, J.J., Tannock, I.F.** 2005. Repopulation of cancer cells during therapy: an important cause of treatment failure. Nat Rev Cancer **5:**516-525.

17. **Kunigal, S., Lakka, S.S., Joseph, P., Estes, N., Rao, J.S.** 2008. Matrix metalloproteinase-9 inhibition down-regulates radiation-induced nuclear factor-kappa B activity leading to apoptosis in breast tumors. Clin Cancer Res **14:**3617-26.
18. **Kunnumakkara, A.B., Diagaradjane, P., Guha, S., Deorukhkar, A., Shentu, S., Aggarwal, B.B., Krishnan, S.** 2008. Curcumin sensitizes human colorectal cancer xenografts in nude mice to gamma-radiation by targeting nuclear factor-kappaB-regulated gene products. Clin Cancer Res **14:**2128-36.
19. **Lamson, D.W., and Plaza, S.M.** 2003. The anticancer effects of vitamin K. Altern Med Rev **8:**303-18.
20. **Magné, N., Toillon, R.A., Bottero, V., Didelot, C., Houtte, P.V., Gérard, J.P., Peyron, J.F.** 2006. NF-kappaB modulation and ionizing radiation: mechanisms and future directions for cancer treatment. Cancer Lett **231:**158-68.
21. **Marc, S.R., Kenneth R.B., Gary, K.R., Muschel, W., Gillies, M.** Ionizing radiation and the cell cycle: A review. Radiat Oncol Investig 1996, **4:**147-158.
22. **Margolin, K.A., Akman, S.A., Leong, L.A., Morgan, R.J., Somlo, G., Raschko, J.W., Ahn, C., Doroshow, J.H.** 1995. Phase I study of mitomycin C and menadione in advanced solid tumors. Cancer Chemother Pharmacol **36:**293-8.
23. **Mayer, H., and Isler, O.** 1971, Methods Enzymol. **18**, 491.
24. **Mizuta, T., Ozaki, I., Eguchi, Y., Yasutake, T., Kawazoe, S., Fujimoto, K., Yamamoto, K.** 2006. The effect of menatetrenone, a vitamin K2 analog, on disease recurrence and survival in patients with hepatocellular carcinoma after curative treatment: a pilot study. Cancer **106:**867-72.
25. **Munday, R., Smith, B.L., Munday, C.M.** 1995. Toxicity of 2,3-dialkyl -1,4-naphthoquinones in rats: comparison with cytotoxicity in vitro. Free Radic Biol Med **19:**759-65.
26. **Munday, R., Smith, B.L., Munday, C.M.** 1999. Effect of inducers of DT-diaphorase on the toxicity of 2-methyl- and 2-hydroxy-1,4-naphthoquinone to rats. Chem Biol Interact **123:**219-37.
27. **Nagendraprabhu, P., Sudhandiran, G.** 2009, Astaxanthin inhibits tumor invasion by decreasing extracellular matrix production and induces apoptosis in experimental rat colon carcinogenesis by modulating the expressions of ERK-2, NF-kappaB and COX-2. Invest New Drugs **Epub ahead of print**.
28. **Nishikawa, Y., Carr, B.I., Wang, M., Kar, S., Finn, F., Dowd, P., Zheng, Z.B., Kerns, J., Naganathan, S.** 1995. Growth inhibition of hepatoma cells induced by vitamin K and its analogs. J Biol Chem **270:**28304-10.
29. **Ogawa, K., Murayama, S., Mori, M.** 2007. Predicting the tumor response to radiotherapy using microarray analysis. Oncol Rep **5:**1243-8
30. **Orlowski, R.Z., Baldwin, A.S.** 2002. NF-kappaB as a therapeutic target in cancer. Trends Mol Med **8:**385-389.
31. **Ozaki, I., Zhang, H., Mizuta, T., Ide, Y., Eguchi, Y., Yasutake, T., Sakamaki, T., Pestell, R.G., Yamamoto, K.** 2007. Menatetrenone, a vitamin K2 analogue, inhibits hepatocellular carcinoma cell growth by suppressing cyclin D1 expression through inhibition of nuclear factor kappaB activation. Clin Cancer Res **13:**2236-45.
32. **Pajonk, F., Pajonk, K., McBride, W.H.** 1999. Inhibition of NF-kappaB, clonogenicity, and radiosensitivity of human cancer cells. J Nath Cancer Inst **91:**1956-60.
33. **Pelicano, H., Feng, L., Zhou, Y., Carew, J.S., Hileman, E.O., Plunkett, W., Keating, M.J., Huang, P.** 2003. Inhibition of mitochondrial respiration: a novel strategy to enhance drug-induced apoptosis in human leukemia cells by a reactive oxygen

species-mediated mechanism. J Biol Chem **278:**37832-9.

34. **Pelicano, H., Xu, R.H., Du, M., Feng, L., Sasaki, R., Carew, J.S., Hu, Y., Ramdas, L., Hu, L., Keating, M.J., Zhang, W., Plunkett, W., Huang, P.** 2006. Mitochondrial respiration defects in cancer cells cause activation of Akt survival pathway through a redox-mediated mechanism. J Cell Biol **175:**913-23.
35. **Sasaki, R., Shirakawa, T., Zhang, Z.J., Tamekane, A., Matsumoto, A., Sugimura, K., Matsuo, M., Kamidono, S., Gotoh, A.** 2001. Additional gene therapy with Ad5CMV-p53 enhanced the efficacy of radiotherapy in human prostate cancer cells. Int J Radiat Oncol Biol Phys **51:**1336-45.
36. **Sasaki, R., Suzuki, Y., Yonezawa, Y., Ota, Y., Okamoto, Y., Demizu, Y., Huang, P., Yoshida, H., Sugimura, K., Mizushina, Y.** 2008. DNA polymerase gamma inhibition by vitamin K3 induces mitochondria-mediated cytotoxicity in human cancer cells. Cancer Sci **99:**1040-8.
37. **Setsukinai, K., Urano, Y., Kakinuma, K., Majima, H.J., Nagano, T.** 2003. Development of novel fluorescence probes that can reliably detect reactive oxygen species and distinguish specific species. J Biol Chem **278:**3170-75.
38. **Shearer, M.J., and Newman, P.** 2008. Metabolism and cell biology of vitamin K. Thromb Haemost. **100:**530-47.
39. **Sibayama-Imazu, T., Fujisawa, Y., Masuda, Y., Aiuchi, T., Nakajo, S., Itabe, H., Nakaya, K.** 2008. Induction of apoptosis in PA-1 ovarian cancer cells by vitamin K2 is associated with an increase in the level of TR3/Nur77 and its accumulation in mitochondria and nuclei. J Cancer Res Clin Oncol **134:**803-12.
40. **Suhara, Y., Murakami, A., Nakagawa, K., Mizuguchi, Y., Okano, T.** 2006. Comparative uptake, metabolism, and utilization of menaquinone-4 and phylloquinone in human cultured cell lines. Bioorg Med Chem **14:**6601-7.
41. **Tsujioka, T., Miura, Y., Otsuki, T., Nishimura, Y., Hyodoh, F., Wada, H., Sugihara, T.** 2006. The mechanisms of vitamin K2-induced apoptosis of myeloma cells. Haematologica **91:**613-9.
42. **Voboril, R., Weberova-Voborilova, J.** 2006. Constitutive NF-kappaB activity in colorectal cancer cells: impact on radiation-induced NF-kappaB activity, radiosensitivity, and apoptosis. Neoplasma **53:**518-23.
43. **Yang, S.Y., Sales, K.M., Fuller, B., Seifalian, A.M., Winslet, M.C.** 2009. Apoptosis and colorectal cancer: implications for therapy. Trends Mol Med **15:**225-33.
44. **Yokoyama, T., Miyazawa, K., Naito, M., Toyotake, J., Tauchi, T., Itoh, M., You, A., Hayashi, Y., Georgescu, M.M., Kondo, Y., Kondo, S., Ohyashiki, K.** 2008. Vitamin K2 induces autophagy and apoptosis simultaneously in leukemia cells. Autophagy **4:**629-40.
45. **Yoshida, T., Miyazawa, K., Kasuga, I., Yokoyama, T., Minemura, K., Ustumi, K., Aoshima, M., Ohyashiki, K.** 2003. Apoptosis induction of vitamin K2 in lung carcinoma cell lines: the possibility of vitamin K2 therapy for lung cancer. Int J Oncol **23:**627-32.
46. **Yoshida, K., Sasaki, R., Nishimura, H., Okamoto, Y., Suzuki, Y., Kawabe, T., Saito, M., Otsuki, N., Hayashi, Y., Soejima, T., Nibu, K., Sugimura, K.** 2009. Nuclear factor-kappaB expression as a novel marker of radioresistance in early-stage laryngeal cancer. Head Neck **Epub ahead of print.**

Enhancement of human cancer cell radiosensitivity by conjugated eicosapentaenoic acid - a mammalian DNA polymerase inhibitor

YUKO KUMAMOTO-YONEZAWA[1], RYOHEI SASAKI[2], YOKO SUZUKI[2], YUKI MATSUI[1], TAKAHIKO HADA[3], KEISUKE URYU[3], KAZURO SUGIMURA[2], HIROMI YOSHIDA[1,4] and YOSHIYUKI MIZUSHINA[1,4]

[1]Laboratory of Food and Nutritional Sciences, Department of Nutritional Science, Kobe-Gakuin University, Nishi-ku, Kobe, Hyogo 651-2180; [2]Division of Radiology, Kobe University Graduate School of Medicine, Chuou-ku Kobe, Hyogo 650-0017; [3]Department of Research and Development, Bizen Chemical Co. Ltd., Akaiwa, Okayama 709-0716; [4]Cooperative Research Center of Life Sciences, Kobe-Gakuin University, Chuou-ku, Kobe, Hyogo 650-8586, Japan

Received September 23, 2009; Accepted November 6, 2009

DOI: 10.3892/ijo_00000532

Abstract. We previously found that conjugated eicosapentaenoic acid (cEPA) selectively inhibited the activities of mammalian DNA polymerases (pols), and suppressed human cancer cell growth. The aim of the present study was to evaluate the efficacy of concurrent radiation with cEPA in a human colon carcinoma cell line, HCT 116. Furthermore, we examined the most effective timing of irradiation. The post-irradiation addition of cEPA significantly enhanced HCT116 cell radiosensitivity by decreasing the expression of pols ß, δ and ε, increasing damaged DNA, such as DNA double-strand breaks, inhibiting clonogenic survival, and inducing apoptosis. However, cells treated by pre-irradiation addition of cEPA did not influence radiosensitive survival and radiation-induced apoptosis. cEPA inhibited the activities of pols needed for DNA repair, thereby DNA damage must be augmented by cEPA and irradiation. These results suggested that the combination of inhibitors of DNA repair-related pols/radiation could be an effective anticancer therapy.

Correspondence to: Dr Yoshiyuki Mizushina, Laboratory of Food and Nutritional Sciences, Department of Nutritional Science, Kobe-Gakuin University, Nishi-ku, Kobe, Hyogo 651-2180, Japan
E-mail: mizushin@nutr.kobegakuin.ac.jp

Abbreviations: cEPA, conjugated eicosapentaenoic acid; pol, DNA polymerase (EC 2.7.7.7); DSB, DNA double-strand break; PUFA, polyunsaturated fatty acid; ATR, ataxia-telangiectasia mutated- and Rad3-related protein kinase; MTT, 3-(4,5-dimethylthiazol-2-yl)-2,5-diphenyltetrazolium bromide; PCR, polymerase chain reaction

Key words: conjugated eicosapentaenoic acid, DNA polymerase, enzyme inhibitor, radiosensitivity, DNA damage, anticancer therapy

Introduction

DNA polymerases (pol, i.e., DNA-dependent DNA polymerases, E.C. 2.7.7.7) catalyze the addition of deoxyribonucleotides to the 3'-hydroxyl terminus of primed double-stranded DNA molecules, and are involved in producing vital cellular processes, such as DNA replication, repair and recombination (1). The human genome encodes at least 15 pols to conduct cellular DNA synthesis (2,3). Eukaryotic cells contain three replicative pols (α, δ and ε), mitochondrial pol γ, and at least 13 repair-related pols; ß, δ, ε, ζ, η, θ, ι, κ, λ, μ, ν, terminal deoxynucleotidyl transferase (TdT) and REV1 (2-4). Pols have recently emerged as important cellular targets for chemical intervention in the development of anticancer agents.

We have been screening for pol inhibitors from natural products (5,6), and found that mammalian pols α and ß are inhibited by linear-chain fatty acids with the following characteristics: 1) C18- or more carbon chains, 2) a free carboxylic group, and 3) double bonds of *cis*-configuration, n-3 polyunsaturated fatty acid (PUFA) having the strongest inhibitory effect of any fatty acid tested (7,8). Eicosapentaenoic acid (EPA; 5*Z*8*Z*11*Z*14*Z*17*Z*-20:5) and docosahexanoic acid (DHA; 4*Z*7*Z*10*Z*13*Z*16*Z*19*Z*-22:6), both n-3 PUFAs, exert significant inhibitory effects on colon carcinoma cell growth at the primary site and metastases (9,10). PUFA are present at high concentrations in some fish oils, and have been evaluated in various clinical trials in which they have proved to be safe and well tolerated.

Conjugated fatty acids are positional and geometrical isomers with several conjugated double bonds. Fatty acids with conjugated double bonds exist in nature; seaweeds such as red and green algae contain highly n-3 unsaturated conjugated fatty acids, i.e., conjugated eicosapentaenoic acid (cEPA; 5*Z*7*E*9*E*14*Z*17*Z*-20:5), bosseopentaenoic acid (5*Z*8*Z*10*E*12*E*14*Z*-20:5) and stellaheptaenoic acid (4*Z*7*Z*9*E*11*E*13*Z*16*Z*19*Z*-22:7) (11,12). As n-3 PUFAs have been shown to have anticarcinogenic activity, conjugated fatty acids converted from n-3 PUFAs may show higher tumor-

inhibiting activity than n-3 PUFAs themselves (13,14). We previously realized the importance of the two classes of n-3 PUFA; EPA and DHA, normal and conjugated, and the inhibitory effect of cEPA on pols was stronger than that of EPA, DHA and cDHA (15). Furthermore, cEPA regulates the cell cycle by DNA damage-response proteins, including the ataxia-telangiectasia mutated- and Rad3-related protein kinase (ATR)-Chk1/2 pathway without influencing the proliferation of normal cells (16,17).

Radiotherapy is one of the most commonly used therapeutic modalities in cancer treatment. Radiation ionizes the molecules of tumor cells, and damages their DNA (18). These effects are not limited to tumor cells but also affect normal cells within the tumor stroma (19,20). The cytotoxicity of radiation is mostly mediated through the generation of DNA double-strand breaks (DSBs) as demonstrated by the radiosensitivity of cells and organisms defective in the machinery of DSB repair (21-23). Ataxia-telangiectasia mutated (ATM) protein kinase is a component of these pathways and integrates the cellular response to damage by phosphorylating some key proteins involved in cell cycle regulation and DSB repair (24,25). Thus, cEPA seems to be an ideal model for the study not only of the molecular mechanisms that inhibit pol activity for the development of new anticancer drugs, but also of cellular proliferation processes such as DNA replication and repair of damaged DNA, such as DSBs, by X-ray irradiation.

In the present study, we investigated whether the radiosensitizing effect of cEPA on human colon carcinoma HCT116 cells and further analyzed the mechanisms of radiosensitization by cEPA.

Materials and methods

Materials. EPA was purchased from Nu-Chek Prep Inc. (Elysian, MN, USA). Nucleotides and chemically synthesized DNA template primers, such as poly(dA) and oligo(dT)$_{12-18}$, and radioisotope reagents, such as [^{3}H]-dTTP (2'-deoxythymidine 5'-triphosphate) (43 Ci/mmol), were purchased from GE Healthcare Bio-Science Corp. (Piscataway, NJ, USA). All other reagents were of analytical grade and purchased from Nacalai Tesque Inc. (Kyoto, Japan).

Preparation of cEPA by alkaline treatment. cEPA was prepared by alkaline treatment following the AOAC method with slight modifications (26). Potassium hydroxide at a concentration of 6.6 or 21% (w/w) in ethylene glycol was prepared and the KOH solution was bubbled for 5 min with nitrogen gas. EPA (10 mg) was added to 1 ml of 6.6% or 21% KOH solution in a test tube (10 ml volume). The mixture was bubbled with nitrogen gas and then screw-capped and allowed to stand for 5 or 10 min at 180˚C. The reaction mixture was cooled, and 1 ml methanol was added. The mixture was acidified to below pH 2 with 2 ml of 6 N HCl. After dilution with 2 ml distilled water, the conjugated fatty acid was extracted with 5 ml hexane. The hexane extract was then washed with 3 ml of 30% methanol and with 3 ml distilled water before being evaporated under a nitrogen gas stream. The conjugated fatty acids were stored at -20˚C after being purged with nitrogen gas. UV/VIS spectrophotometric analysis was performed with a Shimadzu UV-2400PC. Spectrophotometric readings confirmed the conjugation of fatty acids of pentaene (345 nm) (27). cEPA was dissolved in dimethyl sulfoxide (DMSO) at various concentrations and sonicated for 30 sec.

Cell culture. Human colon carcinoma cell line, HCT116, was a kind gift from Dr Bert Vogelstein (Johns Hopkins University, Baltimore). The cells were maintained in McCoy's 5A medium supplemented with 10% FBS, sodium bicarbonate (2 mg/ml) and streptomycin (100 μg/ml) at 37˚C in a humidified atmosphere of 5% CO_2/95% air.

MTT (3-(4,5-dimethylthiazol-2-yl)-2,5-diphenyltetrazolium bromide) assay. HCT116 cells were trypsinized and resuspended in McCoy's 5A medium with 10% FBS, and $5x10^3$ cells were seeded in 96-well tissue culture plates for 24 h. The cells were then stimulated with different concentrations of cEPA containing DMSO of final concentration of 1% for 24 h. After treatment, MTT solution was added (final concentration 0.5 mg/ml MTT in PBS) for 3 h (28). The medium was discarded and the cells were lysed in acidified 2-propanol. Absorbance was measured at 570 nm on a microplate reader (Molecular Devices, Sunnyvale, CA, USA).

DNA polymerase assay of the cell extract. HCT116 cells were plated at $3x10^5$ into a 100-mm culture dish with or without 30 μM of cEPA. After 24 h incubation, the cells were washed with PBS, collected by centrifugation, and the pellets were sonicated for 3 min in lysis buffer (10 mM NaCl, 10 mM Tris-HCl, 1 mM EDTA, 1.5 mM $MgCl_2$, 1 mM dithiothreitol, 7.5% glycerol, 1% Triton X). The pol activity of the cell extract was measured as described previously (7,8). Poly(dA)/oligo(dT)$_{12-18}$ and dTTP were used as the DNA template-primer and nucleotide substrate, respectively. One unit of pol activity was defined as the amount of enzyme that catalyzed the incorporation of 1 nmol dNTP (2'-deoxyribonucleotide 5'-triphosphate, i.e. dTTP) into the synthetic DNA template-primers [i.e. poly(dA)/oligo(dT)$_{12-18}$, A/T=2/1] in 60 min at 37˚C under normal reaction conditions for the enzyme (7,8).

X-ray irradiation. Cultures of HCT116 cells were irradiated using an X-ray irradiator (MBR-1505R2; Hitachi Medico, Tokyo, Japan) at a dose rate of 7.8 Gy/min. Dosimetry was carried out using an ionization chamber connected to an electrometer system.

Real-time PCR analysis. Real-time polymerase chain reaction (PCR) analyses were conducted using standard assays according to Heintel *et al* (29). HCT116 cells were pre-cultured for 24 h, treated with or without 30 μM cEPA for 24 h, radiated at 8 Gy X-ray and subsequently incubated for 10 min. Total RNA was isolated from treated HCT116 cells using the RNeasy mini kit (Qiagen, Hilden, Germany). The extracted total RNA was reverse-transcribed into single-stranded cDNA using a High Capacity RNA-to-cDNA Kit (Applied Biosystems, Warrington, UK). Aliquots of cDNA were used as templates for real-time PCR reactions containing

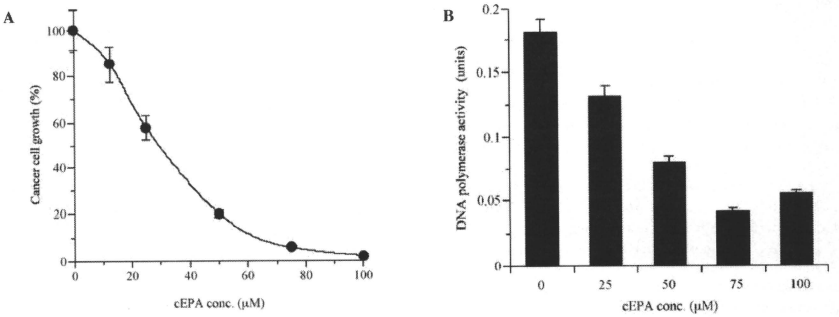

Figure 1. Inhibitory effect of cEPA on the proliferation of HCT116 cells. (A) Dose-response curves of growth inhibition on human colon carcinoma cell line, HCT116 incubated with various concentrations of cEPA for 24 h. Cell proliferation was determined by MTT assay (28). Values are shown as the means ± SEM of three independent experiments. (B) Total pol activity of cell-free extracts from HCT116 cells incubated with cEPA. HCT116 cells ($3x10^5$ cells) were incubated with the indicated concentrations of cEPA for 24 h. From the cell extracts, total pol activity was measured as described previously (7,8). One unit of pol activity is defined as the amount that catalyzes the incorporation of 1 nmol dexyribonucleoside triphosphate (i.e., dTTP) into synthetic template-primers [i.e., poly(dA)/oligo$(dT)_{12\text{-}18}$, A/T=2/1] at 37°C in 60 min. Values are the means ± SEM of four independent experiments.

primers of either the target gene or the control. All oligonucleotide primers for the endogenous control (*18s rRNA*) and the target five pol genes (i.e., human pols α, ß, δ, ε and λ) were synthesized by Applied Biosystems, and were as follows: accession number (*common name*), 4308329 (*18s rRNA*); Hs00415835 (*polymerase α*); Hs00160263 (*polymerase ß*); Hs00172491 (*polymerase δ*); Hs00173030 (*polymerase ε*); Hs00203191 (*polymerase λ*). Each amplification was performed using first-strand cDNA with TaqMan First Universal PCR Master Mix (Applied Biosystems). The PCR reactions, TaqMan analyses, and subsequent calculations were performed with the StepOne™ Real-Time PCR System (Applied Biosystems) according to the manufacturer's instructions. All reactions were performed in a 20 μl reaction volume in triplicate. The mRNA expression level was determined using the $2^{-\Delta CT}$ method.

Comet assay. To assess the generation of DSB in cultured cancer cells, the standard protocol for the single-cell electrophoresis (comet) preparation and analysis was adopted (30). Briefly, HCT116 cells were seeded, cultured in 6-well plates for 24 h, and then incubated with or without 30 μM cEPA for 30 min. The plates were immediately radiated with 8 Gy X-ray. After the irradiated cells with or without cEPA were harvested for 0, 15 and 30 min, the cells were lysed in neutral (pH 7.0) buffer, electophoresed, and stained following the manufacturer's instructions. For evaluation of DNA damage, 500 cells/subject were analyzed at x400 magnification under a fluorescent microscope (BX51N-34-FL; Olympus Corp., Tokyo, Japan) equipped with a 540 nm excitation filter and a 590 nm barrier filter. The mean % tail DNA was analyzed using the imager Rainbow Star (RBS-111; Toyobo Co., Tokyo, Japan).

Radiation clonogenic assay. Survival following radiation exposure was defined as the ability of cells to maintain clonogenic capacity and form colonies. After HCT116 cells were treated with vehicle (DMSO) alone, cEPA alone, irradiation alone, or cEPA plus irradiation for 48 h, the cells were trypsinized, counted, and appropriate dilutions were made. The appropriate number of cells was plated in fresh medium without cEPA for colony formation into 100 mm dishes. After incubation intervals of 14 days, the colonies (containing ≥50 cells) were stained with methylene blue, and the numbers of colonies were counted. The surviving fraction (SF) was calculated as a ratio of the number of colonies to the number of cells plated (plating efficiency) divided by the same ratio calculated for the non-irradiated group. Experiments were performed in duplicate.

Assessment of apoptosis by annexin V staining. Exactly 48 h after treatment with cEPA (30 μM) alone, irradiation (8 Gy) alone, or cEPA/radiation combination, HCT 116 cells were harvested, and then apoptotic cells were detected by annexin V staining using a commercially available kit (PharMingen Annexin V-FITC Apoptosis Detection Kit I; BD Biosciences, San Jose, CA, USA) according to the manufacturer's instructions. The stained cells, which are apoptotic, were analyzed using a FACSCanto II flow cytometer in combination with FACSDiVa software (BD Biosciences).

Results

The effect of cEPA on cellular growth and DNA polymerase activity. First, to determine the effects of cEPA on cultured human cancer cells, we tested their influence on cell growth in human colon carcinoma HCT116 cells. cEPA efficiently inhibited cell growth in a dose-dependent manner, and the LD_{50} value was 30.1 μM for 24 h incubation (Fig. 1). The total pol activity of the HCT116 cell extract, which was treated with cEPA for 24 h, was lower than that of non-treated cells (Fig. 1B). The enzyme activity was dose-dependently

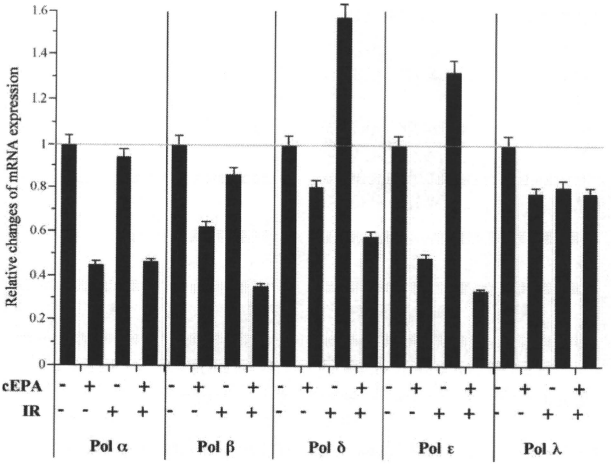

Figure 2. Regulation of pol expression in HCT116 cells by combining cEPA and X-ray radiation. Human colon carcinoma cells (HCT116 cells) were pre-cultured for 24 h, treated with or without 30 μM cEPA for 24 h, radiated at 8 Gy X-ray, and subsequently incubated for 10 min. mRNA was extracted and subjected to real-time PCR as described in Materials and methods. The rate of mRNA expression in both non-treated cEPA and non-irradiated cells (i.e., control) is 1.0. IR is X-ray irradiation. Values are the means ± SEM of three independent experiments.

decreased with an increase in the concentrations of cEPA, and the inhibitory effect of cEPA on cell growth showed the same tendency as that on pol activity in the cells (Fig. 1). Since we previously reported that cEPA selectively inhibited the activities of purified mammalian pols *in vitro* with IC_{50} values of 11.0-31.8 μM (31), the inhibited enzyme by cEPA in the HCT116 cell extract may consist of both DNA replicative pols (i.e., pols α, δ and ε) and DNA repair-related pols (i.e., pols ß, δ, ε and λ). cEPA was more cytotoxic than normal EPA to HCT116 cells, and this tendency of cell growth inhibition was the same as the inhibitory effect of mammalian pols (data not shown).

Effect on expression of pols in HCT116 cells treated with cEPA. Next, we investigated in more detail the effect of cEPA as a selective mammalian pol inhibitor on HCT116 proliferating cells when combined with X-ray radiation. We examined whether the inhibitory activity of pols by 30 μM cEPA/8 Gy radiation combination was associated with the expression of mRNA of pols using real-time PCR. As shown in Fig. 2, 30 μM cEPA (i.e., the LD_{50} value of HCT116 cell growth in Fig. 1A) suppressed the expression of all pols, and especially the mRNA amounts of pols α and ε, which are replicative pols, were less than half against non-treated cEPA (i.e., control). These results suggested that cEPA not only could directly bind to pols and inhibit the activities of pols (31), but also might reduce the expression of pols; therefore, pol inhibition by cEPA must suppress cancer cell proliferation. X-ray radiation-exposed cells strongly increased the mRNA expression level of pols δ and ε, and slightly decreased the mRNA expression level of pols ß and λ. On the other hand, the expressions of pols ß, δ and ε in cells treated with a combination of cEPA and radiation were significantly lower than by radiation alone, and the expression level of pol ε, which catalyzes DNA replication and repair, revealed the most reduced one of these pols investigated.

Inhibitory effect of cEPA on the repair activity of damaged DNA by X-ray radiation. A critical determinant of radiation-induced lethality is the induction and repair of DNA damage, specifically DSBs (32). To determine the effect of cEPA on DNA damage in irradiated HCT116 cells, we evaluated tailing DNA consisting of DSBs by single-cell electrophoresis (comet) assay in neutral buffer. As shown in Fig. 3, in the cells treated with 30 μM cEPA alone, DNA tailing reflecting the formation of DSBs was not observed, suggesting that cEPA does not make DSBs. When cells were exposed to X-rays at 8 Gy alone, DNA tailing was immediately observed in most cells (93.5±7.9%). DNA tailing disappeared gradually with proceeding incubation period, and the cells bearing DNA tailing decreased to 6.4±0.6% at 30 min after irradiation. However, the population of cells bearing DNA tailing, which were treated with a combination of X-rays (8 Gy) and cEPA (30 μM), remained relatively constant 0, 15 and 30 min after irradiation, and the rate of DNA-damaged cells was 94.6±8.2%. These results suggest that HCT116 cells have the ability to quickly repair damaged DNA containing DSBs by X-ray irradiation, and cEPA prevents the repair of damaged DNA by inhibiting the activities of repair-related pols, such as pols ß, δ, ε and λ.